2007

Temporal relationship between renal cyst development, hypertension and cardiac hypertrophy in a new rat model of autosomal recessive polycystic kidney disease

Jacqueline K. Phillips
Murdoch University

Deborah Hopwood
Murdoch University

Rhonda A. Loxley
Murdoch University

Kamaljit Ghatora
University of Sydney

Jason Coombes
Westmead Hospital

See next page for additional authors

Publication Details

Phillips, J. K., Hopwood, D., Loxley, R. A., Ghatora, K., Coombes, J. D., Tan, Y., Harrison, J. L., McKitrick, D. J., Holobotvskyy, V., Arnolda, L. F. & Rangan, G. K. (2007). Temporal relationship between renal cyst development, hypertension and cardiac hypertrophy in a new rat model of autosomal recessive polycystic kidney disease. Kidney and Blood Pressure Research, 30 (3), 129-144.

Temporal relationship between renal cyst development, hypertension and cardiac hypertrophy in a new rat model of autosomal recessive polycystic kidney disease

Abstract

Background/Methods: We have examined the hypothesis that cyst formation is key in the pathogenesis of cardiovascular disease in a Lewis polycystic kidney (LPK) model of autosomal-recessive polycystic kidney disease (ARPKD), by determining the relationship between cyst development and indices of renal function and cardiovascular disease. Results: In the LPK (n = 35), cysts appear at week 3 (1.1 ± 0.1 mm) increasing to week 24 (2.8 ± 2 mm). Immunostaining for nephron-specific segments indicate cysts develop predominantly from the collecting duct. Cyst formation preceded hypertension (160 ± 22 vs. Lewis control 105 ± 20 mm Hg systolic blood pressure (BP), n = 12) at week 6, elevated creatinine (109 ± 63 vs. 59 ± 6 μmol/l, n = 16) and cardiac mass (0.7 vs. 0.4% bodyweight, n = 15) at week 12, and left ventricular hypertrophy (2,898 ± 207 vs. 1,808 ± 192 μm, n = 14) at week 24 (all $p \leq 0.05$). Plasma-renin activity and angiotensin II were reduced in 10- to 12-week LPK (2.2 ± 2.9 vs. Lewis 11.9 ± 4.9 ng/ml/h, and 25.0 ± 19.1 vs. 94.9 ± 64.4 pg/ml, respectively, n = 26, $p \leq 0.05$). Ganglionic blockade (hexamethonium 3.3 mg/kg) significantly reduced mean BP in the LPK (52 vs. Lewis 4%, n = 9, $p \leq 0.05$). Conclusion: Cyst formation is a key event in the genesis of hypertension while the sympathetic nervous system is important in the maintenance of hypertension in this model of ARPKD.

Publication Details

Phillips, J. K., Hopwood, D., Loxley, R. A., Ghatora, K., Coombes, J. D., Tan, Y., Harrison, J. L., McKitrick, D. J., Holobotvskyy, V., Arnolda, L. F. & Rangan, G. K. (2007). Temporal relationship between renal cyst development, hypertension and cardiac hypertrophy in a new rat model of autosomal recessive polycystic kidney disease. Kidney and Blood Pressure Research, 30 (3), 129-144.

Authors

Jacqueline K. Phillips, Deborah Hopwood, Rhonda A. Loxley, Kamaljit Ghatora, Jason Coombes, Ying Sin Tan, Joanne L. Harrison, Douglas J. McKitrick, Vasyl Holobotvskyy, Leonard F. Arnolda, and Gopala K. Rangan

Original Paper

Kidney & Blood Pressure Research

Kidney Blood Press Res 2007;30:129–144
DOI: 10.1159/000101828

Received: October 27, 2006
Accepted: February 6, 2007
Published online: April 19, 2007

Temporal Relationship between Renal Cyst Development, Hypertension and Cardiac Hypertrophy in a New Rat Model of Autosomal Recessive Polycystic Kidney Disease

Jacqueline K. Phillips[a] Deborah Hopwood[b] Rhonda A. Loxley[a]
Kamaljit Ghatora[d] Jason D. Coombes[d] Ying Sin Tan[c] Joanne L. Harrison[a]
Douglas J. McKitrick[c] Vasyl Holobotvskyy[c] Leonard F. Arnolda[c]
Gopala K. Rangan[d]

[a]Division of Health Sciences, School of Veterinary and Biomedical Science, Murdoch University,
[b]Animal Resources Centre, Murdoch, and [c]Cardiology Department, School of Medicine and Pharmacology,
University of Western Australia, Perth, and [d]Centre for Transplant and Renal Research,
Westmead Millennium Institute, The University of Sydney at Westmead Hospital, Sydney, Australia

Key Words
Hypertension · Left ventricular hypertrophy · Cystogenesis · Autosomal-recessive polycystic kidney disease · Renin-angiotensin-aldosterone system · Sympathetic nervous system · Immunohistochemistry

Abstract
Background/Methods: We have examined the hypothesis that cyst formation is key in the pathogenesis of cardiovascular disease in a Lewis polycystic kidney (LPK) model of autosomal-recessive polycystic kidney disease (ARPKD), by determining the relationship between cyst development and indices of renal function and cardiovascular disease. ***Results:*** In the LPK (n = 35), cysts appear at week 3 (1.1 ± 0.1 mm) increasing to week 24 (2.8 ± 2 mm). Immunostaining for nephron-specific segments indicate cysts develop predominantly from the collecting duct. Cyst formation preceded hypertension (160 ± 22 vs. Lewis control 105 ± 20 mm Hg systolic blood pressure (BP), n = 12) at week 6, elevated creatinine (109 ± 63 vs. 59 ± 6 μmol/l, n = 16) and cardiac mass (0.7 vs. 0.4% bodyweight, n = 15) at week 12, and left ventricular hypertrophy (2,898 ± 207 vs. 1,808 ± 192 μm, n = 14) at week 24 (all $p \leq 0.05$). Plasma-renin activity and angiotensin II were reduced in 10- to 12-week LPK (2.2 ± 2.9 vs. Lewis 11.9 ± 4.9 ng/ml/h, and 25.0 ± 19.1 vs. 94.9 ± 64.4 pg/ml, respectively, n = 26, $p \leq 0.05$). Ganglionic blockade (hexamethonium 3.3 mg/kg) significantly reduced mean BP in the LPK (52 vs. Lewis 4%, n = 9, $p \leq 0.05$). ***Conclusion:*** Cyst formation is a key event in the genesis of hypertension while the sympathetic nervous system is important in the maintenance of hypertension in this model of ARPKD.

Introduction

Hypertension is a common and early clinical feature of both autosomal-dominant and -recessive variants of polycystic kidney disease (PKD) [1, 2] and has a major role in the development of left ventricular hypertrophy (LVH) as well as the progression to end-stage renal failure

KARGER

Fax +41 61 306 12 34
E-Mail karger@karger.ch
www.karger.com

1420–4096/07/0303–0129$23.50/0

Accessible online at:
www.karger.com/kbr

Dr. Jacqueline K. Phillips
Division of Health Sciences
School of Veterinary and Biomedical Science, Murdoch University
South St, Murdoch, Perth WA 6150 (Australia)
Tel. +61 8 9360 2257, Fax +61 8 9310 4144, E-Mail j.k.phillips@murdoch.edu.au

[3, 4]. An understanding of the pathogenesis and progression of hypertension is therefore critical to identifying key interventions and limiting morbidity in PKD.

The mechanisms of hypertension in PKD are not well defined and it has been hypothesised that one of the initial precipitants is the development of gross abnormalities in renal structure due to cyst formation causing local tissue ischaemia and the activation of a variety of mediators including the renin-angiotensin-aldosterone system (RAAS), vasoactive peptides and sympathetic nervous system (SNS) [5, 6]. This would suggest that hypertension occurs simultaneously with cyst formation, and precedes development of LVH. Indeed, this is consistent with clinical experience and cross-sectional studies of humans with PKD [5, 7]. The prospective evaluation of this hypothesis in humans is difficult and requires examination in animal models. In that regard, a number of mouse and rat models of PKD are described. In the rat, all known models are the result of spontaneous genetic mutations, while in mice many have been engineered through chemical induction or insertional mutagenesis including targeted mutagenesis of human PKD orthologs [8, for review]. However, to date these models of PKD including the heterozygous Han:SPRD PKD and autosomal-recessive PKD (ARPKD) *wpk* animals show either no or only mild-to-moderate elevations in blood pressure [9–11] and no evidence of progressive cardiovascular disease. Furthermore, genetically engineered mouse models may have specific defects in the cardiovascular system, which may make interpretation complicated [12].

We have examined the overriding hypothesis that cystogenesis is a key event in the pathogenesis of cardiovascular disease in PKD by undertaking a temporal analysis of renal morphology, indices of renal function, blood pressure and cardiac hypertrophy in a new Lewis rat model of PKD (LPK). In order to gain an appreciation of the mechanisms driving hypertension, we have also examined the respective contributions of RAAS and SNS. Preliminary data regarding the LPK model [13] indicates the key trait of marked hypertension from an early age, with inheritance features suggestive of ARPKD. Classically, the cystic lesions in ARPKD arise predominantly from the collecting duct [8] whereas in autosomal-dominant PKD (ADPKD), recent data suggest cysts arise predominantly from the distal nephron [14, 15]. Therefore, in order to determine the site of origin of cysts in the LPK model, we have performed immunohistochemistry to: (1) determine the nephron-segment origin of the cysts, and (2) assess the degree of tubulointerstitial damage, a common histological accompaniment of PKD and predictor of progression.

Materials and Methods

Animals

All experiments were carried out with the approval of the Animal Ethics committees of the respective institutions. Lewis rats with PKD arising as a spontaneous mutation were identified at the Animal Resources Centre, Perth Australia (2002) in a LEW/SsNArc (Lewis) inbred strain originally received from the Department of Health and Human Services, National Institute of Health, USA (1990). The Lewis animals with PKD (LPK) were inbred by brother/sister matings of affected littermates and maintained as an inbred colony. Standard inbred Lewis rats (LEW/CrlBR) bred at the Animal Resources Centre were used as a control strain. The LPK females produced one litter of 8–12 pups at 12–15 weeks of age and did not reproduce again. Animals did not survive beyond 26 weeks of age.

In order to characterise the mode of inheritance, mating experiments were performed. LPK × LPK crossings yielded offspring which all exhibited renal cysts (50 pairs, 345 [100%] polycystic progeny). Brown Norway (BN) × LPK crossings (F1) yielded offspring with no detectable cysts (3 pairs, 3 litters, 18 progeny). For the F1 × F1 crossings (F2; 16 pairs, 16 litters, 152 offspring), 38 developed cystic kidneys (25%, χ^2 value = 0.00, $p < 0.05$). This frequency of PKD in F2 animals supports an autosomal recessive pattern of Mendelian inheritance for a single gene mutation.

Experimental Design and Assessment of Blood Pressure

Whole body and tissue-specific measurements were collected from LPK and Lewis rats at the time points of 3, 6, 12, 16 and 24 weeks of age. At each time point, a minimum of 6 rats (3 female, 3 male) of each strain was used (n = 36 LPK rats, 31 Lewis rats). Prior to CO_2 euthanasia, body weight and tail-cuff blood pressure measurements were made (average of 3 measurements after acclimatization; NIBP controller, ADI Instruments, Castle Hill, NSW, Australia) and voided urine samples collected. Urine was not collected from 3-week-old animals. Immediately following euthanasia, blood was collected by cardiac puncture and wet kidney, heart, pancreas and liver weight recorded. Three other additional groups of animals were used. A group of mixed sex 1-week-old LPK and Lewis rats (n = 6 each strain, total 12 rats) were euthanised and renal tissue collected and processed for morphometric quantification. A group of mixed sex 10- to 12-week-old LPK and Lewis rats (n = 18 and 8, respectively, total 26 rats) were used for collection of blood for plasma-renin activity (PRA), angiotensin II (Ang II) and aldosterone analysis. After stunning and decapitation, blood was collected in chilled tubes containing Na_2 EDTA, the plasma collected and then stored at –80°C until further hormonal analysis. Additional blood was collected for serum urea and creatinine levels. A final group of mixed sex 16-week-old LPK and Lewis rats (n = 4 Lewis, 5 LPK, total 9 animals) were used for ganglionic blockade. Animals were anaesthetised with urethane (Sigma-Aldrich, Mo., USA; 1.2 g/kg i.p.) and a cannula was placed in the femoral artery. The cannula was connected via a bridge amplifier to a Powerlab (AD Instruments) data system. The ganglionic blocking agent hexamethonium bromide (Sigma) was administered subcutaneously (3.3 mg/kg) during continuous measurement of arterial pressure and heart rate. Preliminary studies indicated this dosage as one that produced consistent and tolerated effects in the LPK. Systolic pressure, diastolic pressure,

Table 1. Primary and secondary antibodies used for kidney immunohistochemistry

Primary antibodies	Dilution and source	Secondary antibodies	Antibody target/marker	Indicator
Monoclonal mouse α-rat, clone ED-1, IgG1 Isotype	1:400, Serotec, UK	biotinylated rabbit α-mouse IgG1	monocytes and macrophages/inflammation	tubulointerstitial damage
Monoclonal mouse α-smooth muscle actin (SMA) clone1A4, IgG2a Isotype	1:4,000; Sigma-Aldrich, Sydney, Australia	biotinylated rabbit α-mouse IgG2a	interstitial myofibroblast accumulation	tubulointerstitial damage
Monoclonal mouse α-proliferating cell nuclear antigen (PCNA), clone PC10, IgG2a Isotype	1:100; Dako, Carpinteria, Calif., USA	biotinylated rabbit α-mouse IgG2a	tubular epithelial cell (TEC) proliferation/ inflammation	tubulointerstitial damage
Monoclonal mouse α-vimentin, clone V9, IgG1 Isotype	1:100; Dako, Sydney, Australia	biotinylated rabbit α-mouse IgG1	intermediate filament protein/dedifferentiated epithelia	tubulointerstitial damage
Monoclonal mouse α-rat Aquaporin-1 (AQP1), IgG2b Isotype	1:100; Abcam, Cambridge Science Park, Cambridge, UK	biotinylated goat α-mouse immunoglobulins IgG	proximal convoluted tubule (PCT) and thin descending limb of Henle's loop (DL)	cyst origin
Polyclonal sheep α-Tamm-Horsfall glycoprotein (THG) IgG Isotype	1:200; Chemicon, Boronia, Vic., Australia	biotinylated rabbit α-sheep IgG	thick ascending limb (AL) and distal convoluted tubule (DCT)	cyst origin
Polyclonal rabbit α-rat Aquaporin-2 (AQP2) IgG Isotype	1:100; Abcam	biotinylated goat α-rabbit IgG	cortical and medullary collecting ducts (CD)	cyst origin

mean arterial pressure (MAP) and heart rate were continuously measured until reaching a steady level within 3–5 min of drug administration.

Clinical Biochemistry and Haematology

Full biochemical profiles were performed on animals at weeks 6, 12 and 24. At 3 and 16 weeks, only serum urea and creatinine were determined. Serum creatinine, urea, protein, bilirubin, alkaline phosphatase (ALP), aspartate amino transferase (AST) and alanine amino transferase (ALT) were measured using a Rx Daytona analyser (Randox Laboratories, Antrum, UK). PRA and Ang II levels were determined by radioimmunoassay (ProSearch International Australia, Malvern, Vic., Australia). Plasma aldosterone concentrations were ascertained using a commercially available radioimmunoassay kit (Count a Coat, Diagnostic Products Corporation, California, USA, undertaken by ProSearch International Australia). Micro haematocrit tubes were used to determine packed cell volume (PCV). Urine specific gravity (USG) was measured using a refractometer and urine protein to creatinine ratio determined using a Cobas Mira analyser (Roche Diagnostics, Schweiz, AG).

Tissue Histology

The heart, liver and pancreas were placed into 4% formalin prior to embedding in paraffin wax for histological analysis. Liver, pancreas and a mid-ventricle section of the heart were stained with haematoxylin and eosin (HE) and examined by standard light microscopy. Coronal sections of the kidney were fixed in methyl Carnoy's solution or 4% formalin and after paraffin embedding, 4-μm-thick sections were stained with periodic acid-Schiff (PAS) for cyst morphometric analysis and Gomori's trichrome for histological assessment of collagen deposition.

Immunohistochemistry of the Kidney

To assess the degree of tubulointerstitial damage, and origin of cyst formation, immunohistochemistry using the primary and secondary antibodies as indicated in table 1 was performed. For tubulointerstitial damage, markers for interstitial inflammation (macrophage/monocytes, detected by ED-1 antigen), interstitial myofibroblast accumulation (α-smooth muscle actin, SMA), tubular dedifferentiation (vimentin, an intermediate filament protein expressed in dedifferentiated but not normal epithelia) and tubular epithelial cell (TEC) proliferation (proliferating cell nuclear antigen, PCNA) were used. For determination of cyst origin, the primary antibodies against the following specific nephron segments were used: aquaporin-1 (AQP1) which is a marker for the proximal convoluted tubule and the thin descending limb of Henle's loop [16]; Tamm-Horsfall glycoprotein (THG) which is expressed by the thick ascending limb and distal convoluted tubule [17] and aquaporin-2 (AQP2), whose expression is localised to the apical domains in the principal cells of the cortical and medullary collecting ducts [18, 19].

Primary antibodies were incubated at 4°C overnight, followed by biotinylated species-specific secondary antibodies. All secondary antibodies were used at a dilution of 1:400 and were from Zymed Laboratories (San Francisco, Calif., USA) except for the biotinylated goat anti-mouse immunoglobulins IgG (1:400, Dako, Botany, NSW, Australia). Sections were incubated for 30 min with secondary antibodies. All primary and secondary antibodies were diluted using phosphate buffered saline (PBS; pH 7.4) with 1% bovine serum albumin (BSA) and 1% Tween-20. Immunoreactivity was visualised with Vectastain Elite ABC® reagent (Vector Laboratories, Burlingame, Calif., USA) and the chromogen diaminobenzidine (DAB; Sigma-Aldrich). Methyl-green 2% was used for counterstaining followed by dehydration and application of cover slips using Histomount® (Invitrogen Corporation, Carlsbad, Calif., USA).

Morphometric Quantification of the Kidney

Sections were viewed with a microscope and the images were digitalized using a video camera (BX51/ DP11; Olympus, Perth, WA, Australia) linked to image analysis software (Optimas Image Analysis, Version 5.2; Optimus Corp., Bothell, Wash., USA). A uniformly random cluster method was used to determine microscopic fields for evaluation [20].

To assess cyst formation, cross-sectional diameter of individual cortical cysts was measured using line morphometry, with diameter defined as the length of a straight line joining two points on the cyst circumference. Subjectively, the greatest length possible between two points was taken and the largest cysts within mid-cortical fields assessed. Mean average diameter for each section was determined.

Tubulointerstitial fibrosis was evaluated by quantitative image analysis for percentage area occupied by positive staining for interstitial α-SMA in five mid-cortical fields. Magnification ×200.

Interstitial collagen deposition (Trichrome blue) was assessed semiquantitatively from 0 to 4: 0, absent; 1, <25% of or deposition of interstitial collagen (<25%); 2, 25–50% of or deposition of interstitial collagen (25–50%); 3, 51–75% of or deposition of interstitial collagen (50–75%), and 4, 76–100% of deposition of interstitial collagen (>75%). An average grade was established for each section to determine a mean grade for each time point. Five medullary and five cortical fields from each animal were evaluated (magnification ×200, graticule 0.5 mm^2).

For tubulointerstitial inflammation, ED-1-positive and PCNA-positive interstitial cells were quantified in five midcortical fields measured at ×200. The number of positive cells in each field was counted and an average count was generated for each section. Mean cell counts for each time point were established (cells per mm^2).

For semi-quantitative analysis of tubular vimentin five cortical fields from each animal were examined at ×200 magnification and graded using a score as for collagen deposition. A tubule was defined as positive for vimentin if it contained ≥ one immunoreactive tubular epithelial cell.

Morphometric Quantification of the Heart

A composite image of the heart was taken using a light microscope (LEICA DMBRE, Wetzlar, Germany) and digital camera (NIKON DXM1200F, Nikon Corporation, Kawasaki, Kanagawa, Japan). The assessment of the thickness (μm) of the right ventricular free wall, interventricular septum and left ventricular free wall were determined using Image ProPlus image analysis software (version 4.5.1.29, Media Cybernetics, LP, Md., USA).

Statistical Analyses

Results are presented as means ± SD of combined male and female results unless otherwise stated. All analysis was conducted using the statistical package Statistical Package for the Social Sciences (SPSS; Chicago, Ill., USA). Analysis was performed using a univariate general linear model against the fixed factors of age, strain and sex. Significance was set at $p \leq 0.05$ and the adjusted R^2 (relative predictive powers of the model adjusted for degrees of freedom) provided. For tissue weights, data was converted to percentage body weight. Unless otherwise stated, data was not influenced by blood pressure when entered as a covariate in the model. Level of statistical significance for the effect of strain is provided, and if present, age/strain and/or sex interactions. Results of the univariate analysis drove the Post Hoc analysis, performed using Tukey test ($p \leq 0.05$). The correlation for aldosterone and creatinine was determined in the LPK using a Pearson correlation with a two-tailed test of significance, $p \leq 0.05$.

Results

General Features

The gross phenotype of LPK rats was characterised by progressive nephromegaly (fig. 1a, b). Age, sex and strain all had a significant effect on bodyweight (table 2). There was no macroscopic or microscopic evidence of cyst formation in the liver or pancreas at any age (fig. 1c, d). The weight of the liver was significantly associated with age (proportionally smaller in younger animals) and was only different between the strains at 6 weeks (less in the LPK; table 2). The pancreas showed no significant differences at any age.

LPK Rats Develop Laboratory Abnormalities Consistent with Progressive Kidney Failure

Serum urea was significantly elevated from 3 weeks in LPK rats and serum creatinine by 12 weeks, and both increased with age (table 3). Sex had a significant effect on the levels of urea and creatinine in the LPK animals, with males showing overall higher levels of both markers but there was no age/sex interaction (fig. 2). Urinalysis demonstrated isosthenuria in the LPK rats from week 12 onwards (table 3) and the urine protein: creatinine ratio increased significantly in the LPK animals from 16 weeks of age onwards (table 3; $p \leq 0.05$). At 12 weeks of age, protein (total and albumin) levels were significantly reduced in LPK animals when compared with the Lewis (table 4; $p \leq 0.05$). Globulin levels were reduced in the LPK at 24 weeks of age (table 4; $p \leq 0.05$). Bilirubin and

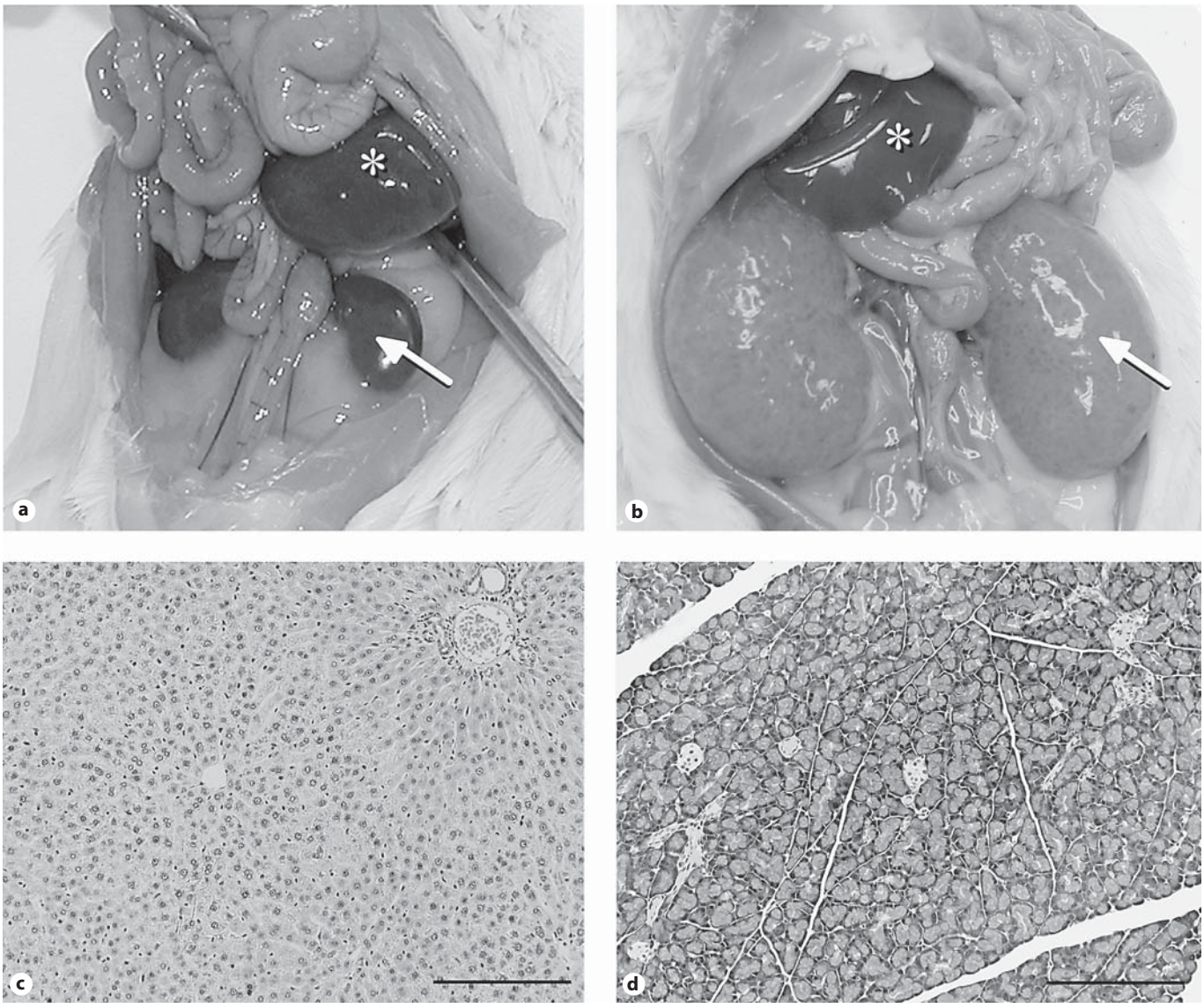

Fig. 1. Gross and microscopic tissue features. In-situ images of kidneys from a 12-week-old Lewis control (**a**) and 12-week-old LPK (**b**) rat. Figure illustrates the dramatic increase in size of the kidneys in LPK (arrow is pointing to left kidney in both panels) and their pale and nodular appearance. Figure also illustrates the normal gross appearance of the liver in the LPK (*). **c**, **d** Light microscopy of histological sections of body tissues stained with HE. **c** shows histologically normal liver tissue from a 24-week-old LPK animal, while **d** shows histologically normal pancreas from a 12-week-old animal LPK. **c**, **d** Scale bar = 200 μm.

the hepatic enzymes ALT and AST did not vary between the strains (table 4). ALP levels showed an age effect, being higher in younger animals, which was more pronounced in the Lewis ($p \leq 0.05$). The PCV was less in the LPK group than age matched Lewis from week 12, and continued to decrease with increasing age (table 4, $p \leq 0.05$). The anaemia was characterised as normocytic and normochromic.

In the group of animals tested for PRA, Ang II and aldosterone, PRA levels were significantly less in the LPK when compared to Lewis at 10–12 weeks of age (2.2 ± 2.9 vs. 11.7 ± 4.9 ng/ml/h, Adj $R^2 = 0.599$, $p < 0.001$, $n = 26$). Angiotensin II levels were also significantly less in the LPK (25.0 ± 19.1 vs. Lewis 94.9 ± 64.4 pg/ml, Adj $R^2 = 0.646$, $p < 0.001$). Angiotensin II levels showed a sex/strain interaction, due to significantly higher levels of Ang II in the male Lewis animals (109.6 ± 17.3 pg/ml, $n = 4$, $p <$

Table 2. Body weight and tissue features in age-matched Lewis and LPK rats

Tissue	3 weeks		6 weeks		12 weeks		16 weeks		24 weeks		Adjusted R^2 value
	$^{(6)}$LEW	$^{(6)}$LPK	$^{(6)}$LEW	$^{(6)}$LPK	$^{(7)}$LEW	$^{(8)}$LPK	$^{(6)}$LEW	$^{(6)}$LPK	$^{(6)}$LEW	$^{(8)}$LPK	
Body, g	66 ± 11	40 ± 3	145 ± 21	160 ± 38	261 ± 75	210 ± 43	303 ± 58	248 ± 63	327 ± 86	237 ± 50	0.96***
Liver, % BW	4.7 ± 0.4	4.5 ± 0.3	5.4 ± 0.3	4.0 ± 0.2	4.2 ± 0.5	3.5 ± 0.4	4.3 ± 0.5	3.5 ± 0.7	3.4 ± 0.7	3.2 ± 0.8	0.91***
Pancreas, % BW	0.4 ± 0.1	0.4 ± 0.1	0.4 ± 0.1	0.3 ± 0.1	0.3 ± 0.1	0.5 ± 0.1	0.3 ± 0.1	0.5 ± 0.0	0.3 ± 0.1	0.5 ± 0.1	0.71
Kidneys, % BW	1.3 ± 0.1	6.5 ± 0.7	1.2 ± 0.05	6.2 ± 2.0	0.9 ± 0.1	8.3 ± 1.2	0.9 ± 0.1	9.6 ± 1.0	0.9 ± 0. 2	9.2 ± 3.5	0.90***

Data represent mean ± SD of combined male and female data. Minimum number of animals in each group indicated by superscript associated with age/strain column. Significance of strain effect: *** $p \leq 0.001$.

Table 3. Biochemical and urological parameters in age-matched Lewis and LPK rats

Parameter	3 weeks		6 weeks		12 weeks		16 weeks		24 weeks		Adjusted R^2 value
	$^{(6)}$LEW	$^{(6)}$LPK	$^{(6)}$LEW	$^{(8)}$LPK	$^{(8)}$LEW	$^{(8)}$LPK	$^{(6)}$LEW	$^{(6)}$LPK	$^{(6)}$LEW	$^{(9)}$LPK	
Urea, mmol/l	5 ± 0.6	13 ± 2	5 ± 0.3	12 ± 4	7 ± 1	34 ± 23	7 ± 0.3	44 ± 18	6 ± 0.7	80 ± 21	0.83***
Creatinine, μmol/l	56 ± 4	30 ± 4	45 ± 2	64 ± 13	59 ± 6	109 ± 63	49 ± 5	150 ± 70	52 ± 5	279 ± 70	0.87***
USG	1.041 ± 0.01	1.039 ± 0.0	1.015 ± 0.01	1.023 ± 0.01	1.029 ± 0.02	1.012 ± 0.0	1.015 ± 0.0	1.011 ± 0.0	1.035 ± 0.01	1.013 ± 0.0	0.50**
Urine Pr:Cr ratio	–	–	2.6 ± 1.4	5.3 ± 3.1	1.1 ± 0.5	5.3 ± 2.6	2.1 ± 1.0	19.2 ± 18.5	1.6 ± 1.2	31.8 ± 22.1	0.50***

Data represent mean ± SD of combined male and female data. Urine specific gravity (USG; isosthenuria range 1.008–1.012), protein:creatinine (Pr:Cr, protein units g/l, creatinine units μmol/l; calculation (8,840) × (urinary protein/urinary creatinine). Minimum number of animals in each group indicated by superscript associated with age/strain column. Significance of strain effect: ** $p \leq 0.01$; *** $p \leq 0.001$.

0.001). Plasma aldosterone levels were not significantly different between the two groups (446.5 ± 442.3 vs. Lewis 412.2 ± 155.8 pg/ml), but there was a wide range in the LPK results. This prompted a correlation analysis that showed aldosterone levels in the LPK were positively correlated with creatinine (Pearson correlation co-efficient 0.607, p = 0.008, n = 18). Creatinine was significantly different between LPK and Lewis in this cohort (73.7 ± 38.3 vs. 46.2 ± 5.7 μmol/l, respectively, $p \leq 0.05$).

Kidney Cysts Arise from the Distal Nephron at Week 3

Kidney weight in LPK rats progressively increased (table 2), with the surface becoming more irregular due to cyst formation. Macroscopically, the reniform shape of

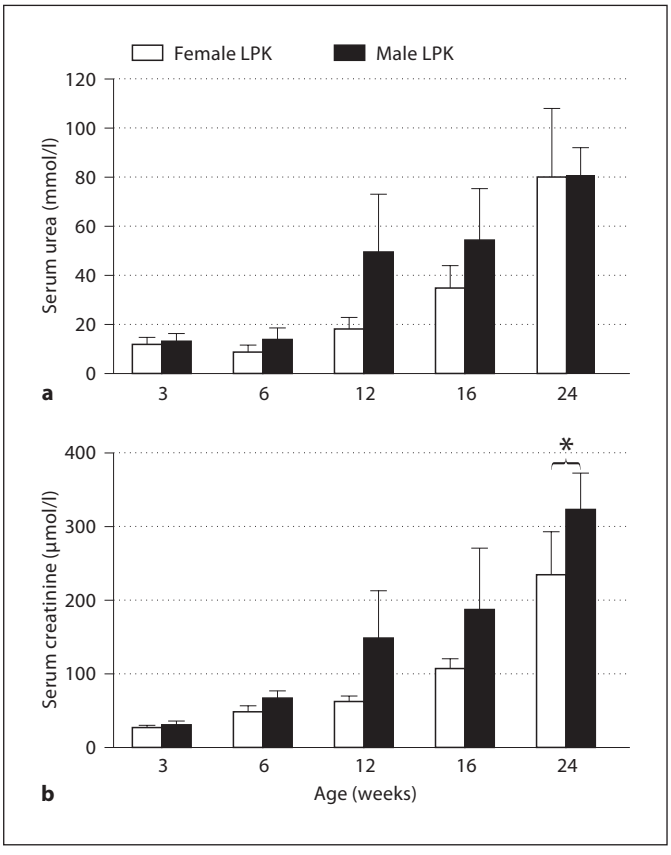

Fig. 2. Graphical representation of elevation in serum urea (**a**) and creatinine (**b**) in male and female LPK animals. Serum urea levels increased with age for both sexes, and while there was no significant difference between males and females at any time point, overall there were significantly higher levels in the male rats (adjusted $R^2 = 0.754$, sex effect p = 0.033). This effect was more pronounced for serum creatinine (**b**; adjusted $R^2 = 0.838$, sex effect $p \leq 0.001$). * Significant difference between males and females at that age, $p \leq 0.05$. Data are means ± SD, n = 37.

Table 4. Biochemical and haematological parameters in age-matched Lewis and LPK rats

Parameter	6 weeks		12 weeks		24 weeks		Adjusted R^2 value
	$^{(6)}$LEW	$^{(6)}$LPK	$^{(6)}$LEW	$^{(7)}$LPK	$^{(6)}$LEW	$^{(8)}$LPK	
Total protein, g/l	60 ± 2	55 ± 3	67 ± 4	57 ± 4	67 ± 9	47 ± 9	0.60***
Albumin, g/l	36 ± 1	34 ± 0.7	40 ± 3	32 ± 2	39 ± 5	28 ± 5	0.67***
Globulin, calc g/l	24 ± 1	22 ± 2	28 ± 2	25 ± 2	25 ± 4	19 ± 4	0.53***
Total bilirubin, μmol/l	2 ± 0.0	4 ± 4	3 ± 1	6 ± 4	2.4 ± 0.7	5 ± 0.8	–0.71
ALT, U/l	121 ± 40	172 ± 168	58 ± 18	116 ± 97	180 ± 142	49 ± 23	0.23
AST, U/l	240 ± 110	488 ± 478	135 ± 67	273 ± 144	242 ± 103	116 ± 53	0.21
ALP, U/l	530 ± 54	343 ± 80	229 ± 53	239 ± 41	200 ± 54	139 ± 39	0.84*
PCV	0.5 ± 0.0	0.4 ± 0.0	0.5 ± 0.0	0.3 ± 0.1	0.5 ± 0.0	0.2 ± 0.1	0.88***

Data represents mean ± SD of combined male and female results. Globulin = Calculated (calc) from total protein and albumin levels. Minimum number of animals in each group indicated by superscript associated with age/strain column. Significance of strain effect: * $p \leq 0.05$; *** $p \leq 0.001$.

the kidney remained intact in LPK animals. The cut surface of the kidney had focal clusters of cysts that were present in the cortex and medulla in the distribution of medullary rays. At week 1, by light microscopy, focal areas of mild dilatation of proximal and distal tubules were present, but cysts were absent (fig. 3a). By week 3, epithelial cell-lined cysts appeared throughout the cortex and medulla (fig. 3b) and the size increased progressively from 12 weeks (fig. 3c–f). Cysts were lined by cuboidal and flattened cells and resembled epithelia from distal nephron segments. Immunostaining for nephron-specific markers indicated that the majority of cysts stained strongly and consistently for aquaporin-2 (fig. 4a, b). In addition, some cells in the cysts stained positive for Tamm-Horsfall protein (THP; fig. 4c, d) and occasionally medullary (but not cortical) cysts were positive for aquaporin-1 (fig. 4e, f), indicating that cysts arose predominantly from the collecting ducts and to a lesser extent from the distal convoluted tubule, thick ascending or thin descending limbs of the nephron.

Cyst Formation Is Associated with Tubule Cell Proliferation/Dedifferentiation and Progressive Tubulointerstitial Inflammation and Fibrosis

The number of PCNA-positive cortical tubule cells was significantly greater in the LPK rats (fig. 5). Similarly, the number of vimentin-positive cortical tubule cells was higher in affected LPK rats at all time points, significantly increasing to week 12 (table 5). The number of interstitial ED-1-positive cells was significantly higher in the LPK animals at 6 and 12 weeks ($p \leq 0.05$; table 5). Diffuse collagen deposition within the renal parenchyma was significantly different to the Lewis from week 12 onwards, increasing further at 24 weeks ($p \leq 0.05$, table 5). Collagen deposition accompanied areas of tubular atrophy, glomerulosclerosis and/or areas dense in dedifferentiated epithelial cells. Use of blood pressure as a covariate in the analysis indicated that collagen deposition in the cortex and medulla was significantly associated with blood pressure ($p = 0.005$, 0.018, respectively). Interstitial myofibroblast accumulation (α-SMA) was significantly higher in the LPK animals relative to age-matched controls from week 6 ($p \leq 0.05$; table 5).

Hypertension Develops Early in LPK, Preceding Cardiac Hypertrophy, and Is Abrogated by Ganglionic Blockade

Tail cuff systolic blood pressures were elevated in LPK rats from week 6 onwards (fig. 6a). Proportional heart weight decreased in the Lewis and LPK between 3 and 6 weeks, but then increased in the LPK, becoming significantly greater than the Lewis from 12 weeks of age (fig. 6b). Proportional LPK heart weights were significantly associated with blood pressure when entered as a covariate in the model ($p = 0.034$, adjusted $R^2 = 0.351$). Hearts from the LPK rats showed no cysts (fig. 6c), but histological examination showed LVH, multifocal muscle degeneration, mild fibrosis, medial hypertrophy of cardiac vessels and increased perivascular mast cell infiltration. Measurements of the left ventricular free wall confirmed LVH in the LPK at 24 weeks of age when compared to Lewis (fig. 6d). The interventricular septum was also significantly thicker in the LPK animals than aged matched Lewis at 24 weeks of age (2,096 ± 178 vs. 1,370 ± 188 μm,

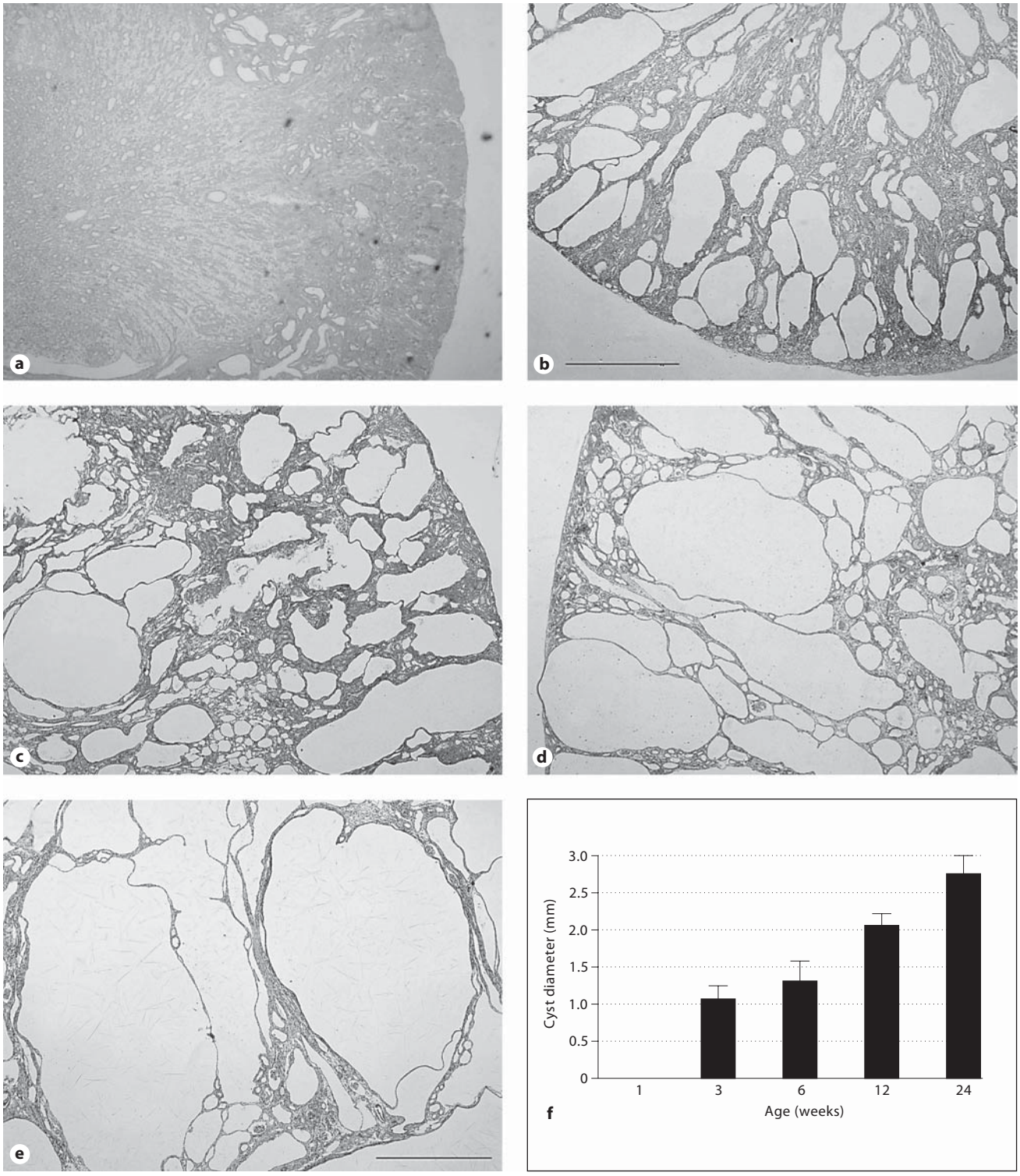

Fig. 3. Cyst development in the LPK animals. **a–e**: Light microscopy of PAS sections of LPK kidneys from animals aged 1 week (**a**), 3 weeks (**b**), 6 weeks (**c**), 12 weeks (**d**) and 24 weeks (**e**). Figures illustrate absence of cysts in the first postnatal week (**a**) although focal areas of dilated proximal and distal convoluted tubules were present. At week 3 there was a rapid appearance of cysts throughout the cortex and medulla (**b**) and these cysts continued to increase in size as the animals aged (**b–e**). **a–e** Scale bar = 1.0 mm. **f** Cyst diameter (mm) as measured using line morphometry. After their appearance in week 3, the size of the cysts increased progressively from 12 weeks onwards ($p \leq 0.05$, adjusted $R^2 = 0.916$). Data are means ± SD. n values are presented in table 5.

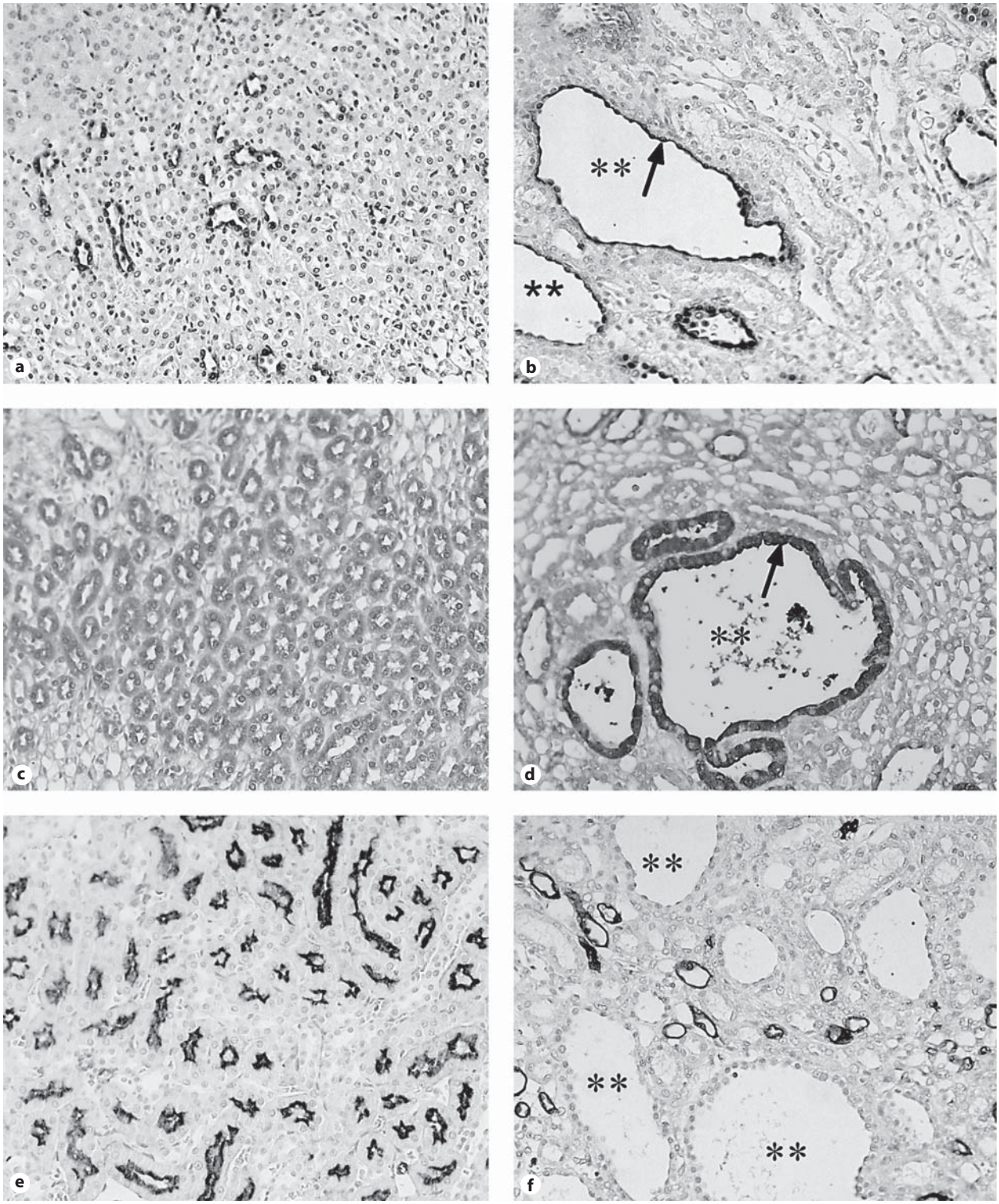

Fig. 4. Immunohistochemical staining of kidney sections for aquaporin-2 (**a**, **b**, medulla), Tamm-Horsfall protein (**c**, **d**, medulla) and aquaporin-1 (**e**, **f**, cortex) in Lewis control (**a**, **c**, **e**) and LPK (**b**, **d**, **f**) animals at week 3. Epithelial cells lining cysts (**) stained positive for aquaporin-2 (predominantly) and to a lesser extent Tamm-Horsfall protein (shown by arrows), but were rarely positive for aquaporin-1. Results therefore indicate that cysts arise predominantly from collecting ductules and the distal nephron. Original magnification ×200.

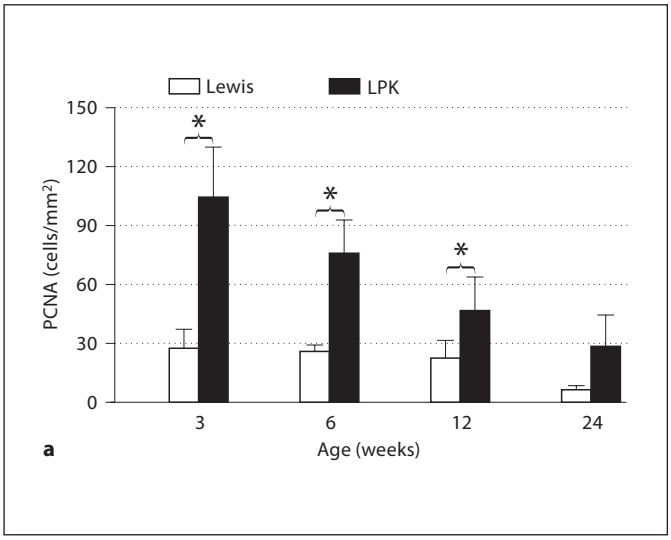

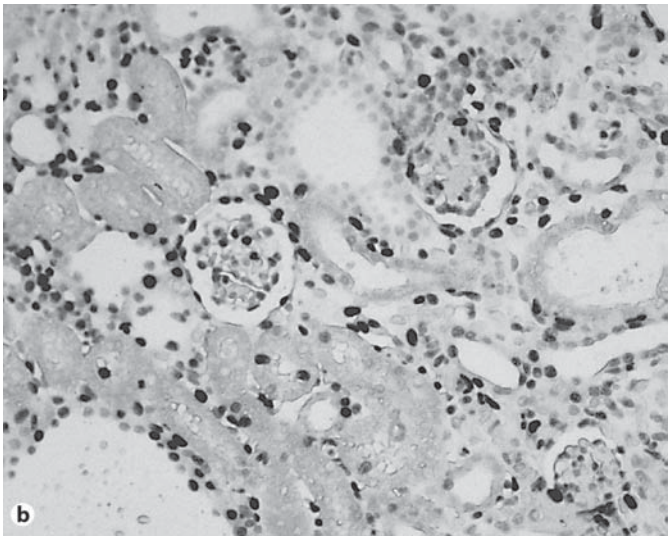

Fig. 5. Cortical tubular epithelial cell (TEC) proliferation as evaluated by proliferating cell nuclear antigen (PCNA) staining. **a** Number of positive cells expressed as cells per mm^2. There were significantly greater numbers of cells in the LPK relative to age-matched Lewis controls at 3, 6 and 12 weeks of age. * Significant difference between LPK and Lewis at that age, $p \leq 0.05$. There was no significant difference between the Lewis at any age, but the 3- and 6-week-old LPK groups were significantly different to each other, and all other LPK age groups (adjusted $R^2 = 0.854$, strain effect $p \leq 0.001$). Data are means ± SD; n values are in table 5. **b** PCNA staining from a 3-week-old PKD. Original magnification ×200.

Table 5. Quantification of renal histopathological parameters in age-matched Lewis and LPK rats

Parameter	1 week		3 weeks		6 weeks		12 weeks		24 weeks		Adjusted R^2 value
	$^{(6)}$LEW	$^{(6)}$LPK	$^{(6)}$LEW	$^{(6)}$LPK	$^{(6)}$LEW	$^{(6)}$LPK	$^{(7)}$LEW	$^{(7)}$LPK	$^{(6)}$LEW	$^{(10)}$LPK	
Vimentin, cor[a]	0.3 ± 0.2	1.4 ± 0.5	0.1 ± 0.1	3.0 ± 0.4	0.2 ± 0.2	3.3 ± 0.8	0.2 ± 0.2	3.9 ± 0.1	0.2 ± 0.2	4.0 ± 0.1	0.97***
ED-1/mm^2 [b]	9.3 ± 0.9	14.0 ± 5.6	5.1 ± 1.1	14.0 ± 2.6	6.0 ± 1.4	34.1 ± 20.3	6.7 ± 1.4	32.6 ± 22.7	8.8 ± 6.8	20.9 ± 13.8	0.44***
Collagen, cx[a]	0.0 ± 0.1	0.2 ± 0.2	0.0 ± 0	0.03 ± 0.1	0.1 ± 0.1	0.23 ± 0.2	0.26 ± 0.2	1.3 ± 0.4	0.4 ± 0.2	2.5 ± 0.5	0.93*
Collagen, med[a]	0.1 ± 0.1	0.1 ± 0.1	0.0 ± 0.0	0.1 ± 0.2	0.1 ± 0.1	0.0 ± 0	0.1 ± 0.1	0.6 ± 0.3	0.1 ± 0.1	1.8 ± 0.5	0.89***
α-SMA[c]	5.0 ± 1.2	3.6 ± 1.1	1.1 ± 0.3	3.6 ± 2.4	1.2 ± 0.6	9.7 ± 2.9	1.1 ± 0.6	10.0 ± 3.5	0.8 ± 0.3	12.2 ± 2.3	0.82**

Data represent mean ± SD of combined male and female data.

[a] Tubular vimentin staining and collagen deposition was scored with arbitrary units for the cortex (cx) or medulla (med).

[b] Immunoreactivity for ED-1 was measured as number of immunoreactive cells in midcortical fields per mm^2.

[c] α-Smooth muscle actin (α-SMA) measured as % of cortical area occupied by positive staining for α-SMA.

Minimum number of animals in each group indicated by superscript associated with age/strain column. Significance of strain effect: * $p \leq 0.05$; ** $p \leq 0.01$; *** $p \leq 0.001$.

respectively, $p \leq 0.05$, adjusted $R^2 = 0.720$, strain effect $p \leq 0.001$). There was no difference between strains for right ventricular free wall thickness (data not shown).

In anaesthetised animals, ganglionic blockade had no significant effect on the Lewis blood pressures (table 6) but it significantly reduced both systolic and diastolic arterial pressures in the LPK, reducing systolic values to pressures comparable to the Lewis, and reducing diastolic values to pressures less than the Lewis (in either the presence or absence of hexamethonium; $p \leq 0.05$), indicating a greater relative drop in diastolic pressures. These changes were reflected by the change in MAP (average fall of 4% in the Lewis and 53% in the LPK). There was no difference between pre- and post-hexamethonium heart rates in either strain.

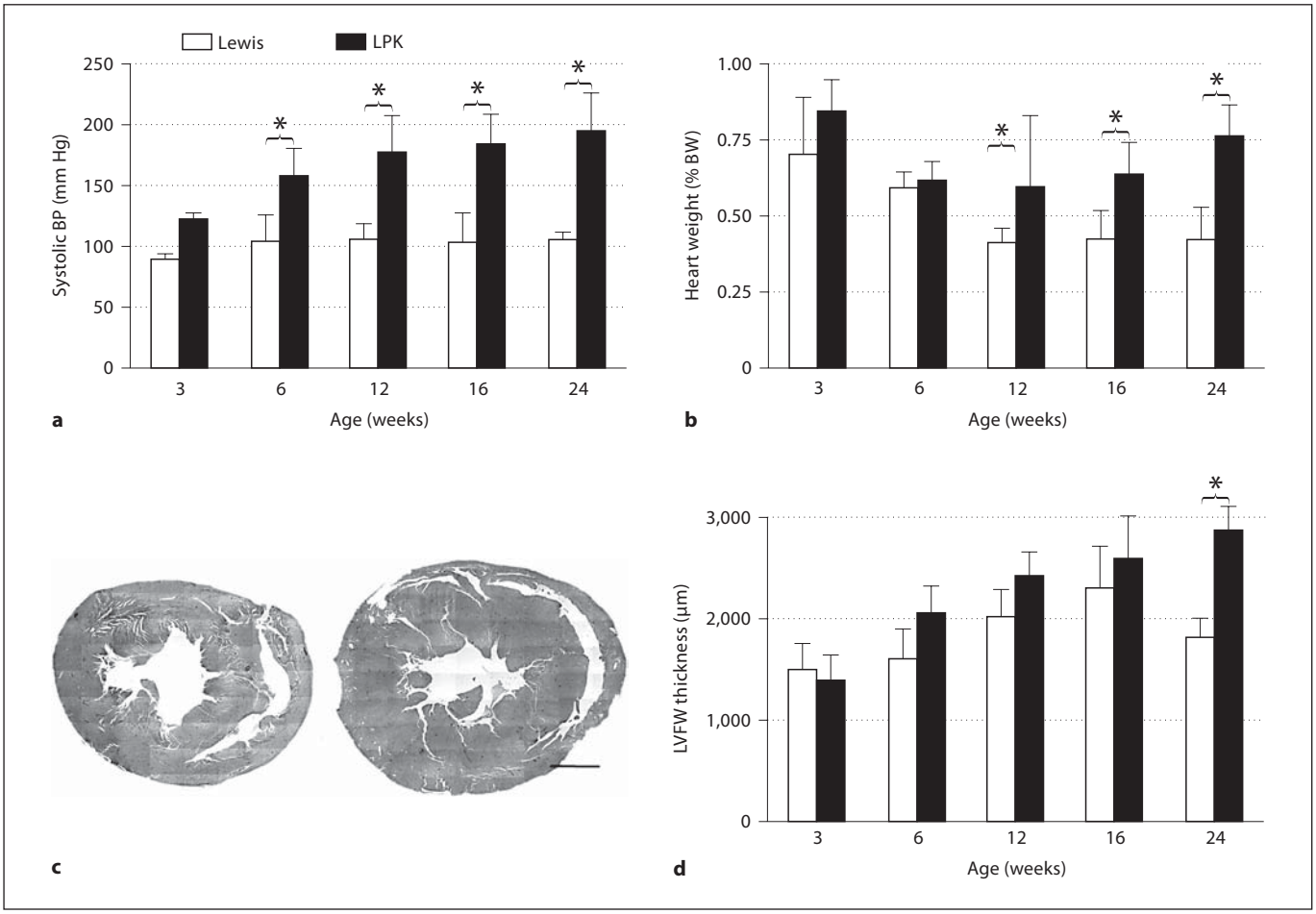

Fig. 6. Hypertension and development of left ventricular hypertrophy. **a** Systolic blood pressure (BP; mm Hg, as measured by tail cuff) and early and sustained presence of hypertension in the LPK animals as compared to Lewis control from week 6 ($p \leq 0.05$, adjusted $R^2 = 0.808$, strain effect $p \leq .001$). There was no significant difference in blood pressure between the Lewis animals at any age nor between the 6-, 12-, 16- and 24-week-old LPK. **b** Heart weight data as a percentage of body weight (% BW) and significant difference between LPK and Lewis animals from 12 weeks of age ($p \leq 0.05$, adjusted $R^2 = 0.86$, strain effect $p \leq 0.001$). There was no difference between Lewis animals at 6, 12, 16 and 24 weeks of age and there was no difference between the LPK animal at 6, 12, 16 and 24 weeks of age. **c** Transverse sections of rat hearts from a 24-week-old Lewis (left) and a 24-week-old LPK (right), and difference in size of the hearts. **c** Scale bar = 2 mm. **d** Thickness of left ventricular free wall (LVFW; μm) and the development of left ventricular hypertrophy in the LPK animals at 24 weeks of age ($p \leq 0.05$, adjusted $R^2 = 0.836$, strain effect $p \leq 0.05$). Age has a significant effect on LVFW thickness in both strains ($p \leq 0.001$). * Significant difference between LPK and Lewis at that age, $p \leq 0.05$. Data are means ± SD, n values are as presented in table 2.

Discussion

In this study we investigated the relationship between cyst formation and indicators of renal function and cardiovascular disease in a new rat model of autosomal-recessive PKD. Our data demonstrate that cyst formation preceded the development of hypertension, which in turn heralded significant increases in serum urea and creatinine, increased cardiac mass and LVH, and eventual end stage renal disease. A key finding was evidence for a suppressed renin angiotensin system and heightened sympathetic drive during the established phases of the disease. These finding therefore support the hypothesis that renal structural abnormalities are a key event in the genesis of hypertension and subsequent target organ disease in PKD. Given that the most important mechanism of limiting renal disease progression is adequate blood pressure control [21], an understanding of the temporal relation-

Table 6. Blood pressure and heart rate response to ganglionic blockade

	Lewis		LPK		Adjusted R^2 value
	pre-Hex	post-Hex	pre-Hex	post-Hex	
Systolic AP, mm Hg	111 ± 8	104 ± 7	178 ± 19	84 ± 13*	0.88
Diastolic AP, mm Hg	64 ± 9	65 ± 7	88 ± 4	41 ± 2*	0.90
Mean AP, mm Hg	80 ± 8	77 ± 6	118 ± 8	56 ± 5*	0.92
Heart rate, bpm	270 ± 39	250 ± 29	326 ± 36	292 ± 28	0.37

Data represent mean ± SD of combined data from animals of mixed sex aged 16 weeks. Arterial pressures (AP) were measured from rats under urethane anaesthesia pre- and post-treatment with the ganglionic blocker hexamethonium (Hex, subcutaneous, 3.3 mg/kg). Significant difference between pre- and post-treatment values: * $p \leq 0.05$; $n = 9$.

ship between cystogenesis and hypertension is key for providing effective therapeutic interventions.

The breeding analysis presented in this study confirms an autosomal recessive pattern of inheritance for PKD in the LPK model. Autosomal-recessive PKD has been shown to be due to mutations in the *PKHD1* gene [22], and indeed initial identification of the *PKHD1* gene arose from mapping of the *pck* rat model, allowing identification of the human ortholog [23]. The specific genetic mutation and likely role of genetic modifiers, which are significant factors in human ARPKD [24], are not yet known for the LPK model and form the basis for current investigation by our group. Given that the functions and mechanisms of the genes currently known to cause PKD remain unclear, future identification of the responsible gene in this model will provide valuable insight into the pathogenesis of ARPKD in humans [8, 23].

The renal histopathology phenotype described in this study further supports our finding of an autosomal-recessive mode of inheritance. Specifically, kidney enlargement was characterised by maintenance of the normal reniform shape, and cysts were due to fusiform dilatation predominantly of the collecting ducts and to a lesser extent other components of the distal nephron. Other autosomal-recessive forms of rodent PKD, such as the *wpk*, also exhibit predominantly collecting duct-derived cysts [10, 25] and in the spontaneously inherited *cpk* mouse model of ARPKD, embryonic cystic lesions are localised to the proximal tubule [26]. Likewise, in human ARPKD, renal disease is characterised in utero by fusiform dilation of the collecting ducts [22, 23]. This is in contrast to ADPKD, in both humans and murine models, where in general cysts are thought to arise from the tubular portion of the nephron as well as the renal collecting system [22].

Our use of markers to identify cyst origin is substantiated by studies in humans and other rodent models where aquaporins and THP have similarly been used to confirm nephron segment localization of cysts in PKD [10, 19]. Indeed AQP1 and AQP2 belong to a group of proteins which retain their segment-specific discriminatory differential expression even in end stage PKD [27]. With regard to the functional significance of staining for these proteins in cystic epithelia of the LPK model, it has been postulated that increased water permeability mediated by aquaporins could contribute to the pathogenesis of cyst formation by the facilitation of fluid secretion in to the cystic lumen [27, 28]. Any potential role for THP, or uromodulin, however, is difficult to delineate, as the biological role of this mucoprotein is still unclear [28].

Temporal analysis of the renal histopathology indicated three distinct structural-functional phases characterised by: (1) a precursor cystic phase (week 1); (2) a cystic phase (weeks 3–6) characterised by tubular epithelial cell proliferation and dedifferentiation, interstitial inflammation with compensatory preservation of renal function, and (3) a cystic phase characterised by tubulointerstitial fibrosis correlating with progressive renal failure (12 weeks). At week 1 precursor cystic lesions (namely focal dilations of proximal and distal tubules) were present. By week 3, however, the medulla and cortex of the kidney were grossly deranged with the presence of diffuse cystic distal tubular dilatation only of predominantly collecting ductules. Interestingly, in the presence of this gross distortion in renal structure, the serum creatinine was normal but blood pressure was significantly elevated by week 6. Cystic enlargement continued until week 24, but at a much slower rate and preceded the development of the other typical histological features of end-stage renal disease, including interstitial macrophage and myofibro-

blast accumulation, interstitial fibrosis and tubular cell dedifferentiation.

Renal function deterioration in progressive chronic kidney disease eventually leads to end stage renal failure and death. Systemic hypertension and proteinuria, characteristics of the LPK model, are important progression factors underlying all forms of chronic kidney disease [21]. In addition to the described change in serum creatinine, laboratory abnormalities consistent with progression of renal dysfunction, including marked increases in serum urea, isosthenuria, decreased serum protein, increased urinary protein to creatinine ratio and reduced PCV were also evident after week 12. The rate of progression of renal insufficiency in the LPK model resembles the time frame of morbidity for the ARPKD Wistar-chi and *pck* (Crj:CD/SD) models [10, 25, 29, 30]. However, unlike the Wistar-chi, *wpk* or *pck* ARPKD models, and also the heterozygous Han:SPRD ADPKD model, the LPK animals do not exhibit extra-renal pathology [8, 31, 32]. This is also in contrast to human ARPKD, which is characterised by the combination of renal cystic disease, congenital hepatic fibrosis, and the occasional occurrence of pancreatic fibrosis [22].

Of interest was the finding that LPK animals demonstrate gender dependent effects, with male animals showing higher overall elevations in serum urea and creatinine. This is consistent with human PKD and other animal models, where males undergo more rapid disease progression and earlier onset of end stage renal disease [33–35]. Studies in the Han:SPRD rat model suggest that oestrogen has a protective effect that promotes the preservation of renal function through the regulation of mediators of growth and fibrosis [35].

Hypertension is a common finding in both ADPKD and ARPKD in humans [36, 37] and is an important factor that not only accelerates renal failure but also drives a spectrum of cardiovascular changes including LVH [6, 7, 38, 39]. In this study, blood pressure increased after early cystogenesis yet prior to marked increases in indicators of renal function. In this regard, the LPK animals show a strong similarity to human PKD. In ADPKD, 60% of patients develop hypertension before renal function is impaired [1] and in a recent retrospective study looking at ARPKD, hypertension was present in 55% of patients, with nearly all neonatal survivors requiring anti-hypertensive treatment [2]. As described, this is distinct to other rodent models of PKD which show no or only very mild to moderate elevations in blood pressure [9–11, 35].

Several mechanisms have been proposed regarding the pathogenesis of hypertension in PKD, including volume overload associated with an abnormal pressure-natriesis response, activation of the RAAS associated with renal cyst formation and induction of local tissue ischaemia, and increased sympathetic activity [40, 41]. With regard to the RAAS, there is conflict in the literature and it has been variably described as increased, decreased or unchanged [3, 11, 40, 42, 43]. In ARPKD, it has been suggested that affected neonates are actually in a low renin state [2, 10]. In this study, both PRA and Ang II levels were low in LPK rats at 10–12 weeks of age. Markedly elevated systolic pressure and indicators of renal dysfunction at this age would suggest that extracellular fluid volume and total body sodium were likely to be increased [44]. Given that sodium loading and increased arterial pressure reduce renin secretion [45, 46], this may explain the suppressed PRA. The reduced Ang II levels are likely to be linked to the low PRA, as a number of studies have shown that PRA and plasma Ang II are strongly correlated [47, 48] and respond similarly to interventions [48, 49]. However, suppressed renin at this time point does not exclude a role for renin in the early pathogenesis of hypertension. In one-kidney, one-clip Goldblatt hypertension, renin is elevated in the early phase and contributes to the early rise in arterial pressure but once sodium retention occurs and arterial pressure rises the increase in renin subsides and renin is usually suppressed in the chronic phase [50, 51]. Similar observations have been made in heart failure where, in animal models, renin rises early and is suppressed in the chronic state, and humans where renin is raised in de-compensated heart failure and tends to fall in chronic stable disease [52, 53].

Aldosterone levels were variable in the LPK, and while on average not higher than control animals, did show a positive correlation with serum creatinine. The basis of this relationship is not known but a similar wide range of aldosterone levels in the presence of reduced PRA have been described previously in feline PKD [54]. Given renewed interest in the role of aldosterone in renal disease progression [55], further studies to clarify the pathogenesis and therapeutic implications of this finding are warranted.

In humans a number of studies have provided strong evidence for an important link between the observed sympathetic hyperactivity and increased risk of cardiovascular morbidity in PKD [3, 4, 56]. Further, it has been shown that muscle sympathetic nerve activity is increased in hypertensive PKD patients regardless of renal function [3]. In our study, sympathetic blockade was undertaken to gain further information about the role of the SNS in maintaining hypertension in PKD. The amount of hexa-

methonium used was lower than used in other studies ($1/10^{th}$) [57, 58], and while it had no significant effect on the normotensive Lewis controls, it had a pronounced effect on the hypertensive LPK. With the caveat that established hypertension induces vascular medial hypertrophy and a vascular amplifier effect [59], these results nonetheless suggest that maintenance of hypertension in the LPK rat is at least partly dependent on an intact SNS.

A number of mechanisms may drive sympathetic activation in PKD. It has been argued that renal ischaemia due to structural changes stimulates inappropriate activation of the renin-angiotensin system [3, 56], with high circulating levels of Ang II in turn directly stimulating central sympathetic outflow via circumventricular organs that lack a functional blood brain barrier [60, 61]. There is, however, an increasing field of study to suggest that intrarenal ischaemia can modulate sympathetic efferent activity by direct stimulation of renal afferents [3, 5]. For example, in patients with end-stage renal failure, bilateral renal nephrectomy corrects increased muscle sympathetic nerve activity concurrent with a reduction in blood pressure [62], and in animal models of renal failure/injury, dorsal rhizotomy or renal denervation significantly attenuates the degree of hypertension [63–65]. Given our finding of low levels of PRA and circulating Ang II, the LPK model will therefore be a useful tool for future evaluation of these pathophysiological interactions between the renal, sympathetic and cardiovascular systems.

In conclusion, we have examined the temporal relationship between cardiac and renal disease progression in ARPKD, demonstrating that renal structural abnormalities precede the development of hypertension, in turn preceding marked changes in indices of renal dysfunction and cardiac hypertrophy. These data raise further hypotheses, including the role of the RAAS and SNS in disease establishment and progression. It also raises questions as to whether diminution of renal cyst formation with anti-proliferative agents such as mammalian target of rapamycin inhibitors [66] can reduce cardiovascular morbidity by both slowing the development of hypertension as well as direct inhibitory effects on cardiac structure. The key features of the LPK model including the course of disease progression indicate it is a suitable model in which to investigate the kidney-cardiovascular axis and genetic pathogenesis of PKD.

Acknowledgments

The authors acknowledge the expert technical assistance provided by Dr. Chandrika Abeywardana (Animal Resources Centre), Mr. Courtney Reddrop, Ms. Kellysan Powers-Martin, Mr. Jada Yengkopiong, Mr. Michael Slaven and Mr. Gerard Spoelstra (Murdoch University). We thank Dr. Amanda O'Hara and Assoc. Prof. Philip Clark (Murdoch University) for their expert opinions regarding the cardiac histology and clinical biochemistry, and Mr. David Casley (ProSearch) for assistance with the hormonal assays. Financial support was provided by Murdoch University, Animal Resources Centre and research funding from the Medical Research Fund (WA), Fremantle Hospital Research Foundation and the National Health and Medical Research Council (Australia, Grant No. 230500 to G.K.R. and 384708 to J.K.P.).

References

1 Gabow PA, Chapman AB, Johnson AM: Renal structure and hypertension in autosomal dominant polycystic kidney disease. Kidney Int 1990;38:1177–1180.
2 Capisonda R, Phan V, Traubuci J, Daneman A, Balfe JW, Guay-Woodford LM: Autosomal recessive polycystic kidney disease: outcomes from a single-center experience. Pediatr Nephrol 2003;18:119–126.
3 Klein IH, Ligtenberg G, Oey PL, Koomans HA, Blankestijn PJ: Sympathetic activity is increased in polycystic kidney disease and is associated with hypertension. J Am Soc Nephrol 2001;12:2427–2433.
4 Neumann J, Ligtenberg G, Klein IH, Blankestijn PJ: Pathogenesis and treatment of hypertension in polycystic kidney disease. Curr Opin Nephrol Hypertens 2002;11:517–521.
5 Wang D, Strandgaard S: The pathogenesis of hypertension in autosomal dominant polycystic kidney disease. J Hypertens 1997;15:925–933.
6 Ecder T, Schrier RW: Hypertension and left ventricular hypertrophy in autosomal dominant polycystic kidney disease. Expert Rev Cardiovasc Ther 2004;2:369–374.
7 Bardaji A, Martinez-Vea A, Valero A, Gutierrez C, Garcia C, Ridao C, Oliver JA, Richart C: Cardiac involvement in autosomal-dominant polycystic kidney disease: a hypertensive heart disease. Clin Nephrol 2001;56:211–220.
8 Guay-Woodford LM: Murine models of polycystic kidney disease: Molecular and therapeutic insights. Am J Physiol 2003;285:F1034–1049.
9 Al-Nimri MA, Komers R, Oyama TT, Subramanya AR, Lindsley JN, Anderson S: Endothelial-derived vasoactive mediators in polycystic kidney disease. Kidney Int 2003;63:1776–1784.
10 Nauta J, Goedbloed MA, Herck HV, Hesselink DA, Visser P, Willemsen R, Dokkum RP, Wright CJ, Guay-Woodford LM: New rat model that phenotypically resembles autosomal recessive polycystic kidney disease. J Am Soc Nephrol 2000;11:2272–2284.
11 Braun C, Ludicke C, Rebsch W, Gretz N, van der Woude FJ, Rohmeiss P: Autoregulation of renal blood flow and pressure-dependent renin release in autosomal dominant polycystic kidney disease of rats. Nephrol Dial Transplant 1996;11(suppl 6):52–57.

12 Boulter C, Mulroy S, Webb S, Fleming S, Brindle K, Sandford R: Cardiovascular, skeletal, and renal defects in mice with a targeted disruption of the pkd1 gene. Proc Natl Acad Sci USA 2001;98:12174–12179.
13 Phillips JK, Rangan G, Hopwood D, McKitrick DJ: Characterisation of hypertension in a new model of PKD in rats. J Hypertens 2004;22:157S [Abstract].
14 Lantinga-van Leeuwen IS, Dauwerse JG, Baelde HJ, Leonhard WN, van de Wal A, Ward CJ, Verbeek S, Deruiter MC, Breuning MH, de Heer E, Peters DJ: Lowering of pkd1 expression is sufficient to cause polycystic kidney disease. Hum Mol Genet 2004;13:3069–3077.
15 Thomson RB, Mentone S, Kim R, Earle K, Delpire E, Somlo S, Aronson PS: Histopathological analysis of renal cystic epithelia in the pkd2ws25/-mouse model of adpkd. Am J Physiol 2003;285:F870–880.
16 Maunsbach AB, Marples D, Chin E, Ning G, Bondy C, Agre P, Nielsen S: Aquaporin-1 water channel expression in human kidney. J Am Soc Nephrol 1997;8:1–14.
17 Bachmann S, Metzger R, Bunnemann B: Tamm-horsfall protein-mRNA synthesis is localized to the thick ascending limb of Henle's loop in rat kidney. Histochemistry 1990;94:517–523.
18 Kishore BK, Krane CM, Di Iulio D, Menon AG, Cacini W: Expression of renal aquaporins 1, 2, and 3 in a rat model of cisplatin-induced polyuria. Kidney Int 2000;58:701–711.
19 Menezes LF, Cai Y, Nagasawa Y, Silva AM, Watkins ML, Da Silva AM, Somlo S, Guay-Woodford LM, Germino GG, Onuchic LF: Polyductin, the pkhd1 gene product, comprises isoforms expressed in plasma membrane, primary cilium, and cytoplasm. Kidney Int 2004;66:1345–1355.
20 Rangan GK, Pippin JW, Couser WG: C5b-9 regulates peritubular myofibroblast accumulation in experimental focal segmental glomerulosclerosis. Kidney Int 2004;66:1838–1848.
21 Harris DC, Rangan GK: Retardation of kidney failure: applying principles to practice. Ann Acad Med Singapore 2005;34:16–23.
22 Igarashi P, Somlo S: Genetics and pathogenesis of polycystic kidney disease. J Am Soc Nephrol 2002;13:2384–2398.
23 Ward CJ, Hogan MC, Rossetti S, Walker D, Sneddon T, Wang X, Kubly V, Cunningham JM, Bacallao R, Ishibashi M, Milliner DS, Torres VE, Harris PC: The gene mutated in autosomal recessive polycystic kidney disease encodes a large, receptor-like protein. Nat Genet 2002;30:259–269.
24 Harris PC, Rossetti S: Molecular genetics of autosomal recessive polycystic kidney disease. Mol Genet Metab 2004;81:75–85.
25 Lager DJ, Qian Q, Bengal RJ, Ishibashi M, Torres VE: The pck rat: A new model that resembles human autosomal dominant polycystic kidney and liver disease. Kidney Int 2001;59:126–136.
26 Ricker JL, Gattone VH 2nd, Calvet JP, Rankin CA: Development of autosomal recessive polycystic kidney disease in Balb/c-cpk/cpk mice. J Am Soc Nephrol 2000;11:1837–1847.
27 Devuyst O, Burrow CR, Smith BL, Agre P, Knepper MA, Wilson PD: Expression of aquaporins-1 and -2 during nephrogenesis and in autosomal dominant polycystic kidney disease. Am J Physiol 1996;271:F169–183.
28 Bissler JJ, Dixon BP: A mechanistic approach to inherited polycystic kidney disease. Pediatr Nephrol 2005;20:558–566.
29 Inage Z, Kikkawa Y, Minato M, Owada M, Kitagawa T, Ohno K, Kondo K, Ueda Y, Iidaka K: Autosomal recessive polycystic kidney in rats. Nephron 1991;59:637–640.
30 Cowley BD Jr, Gudapaty S, Kraybill AL, Barash BD, Harding MA, Calvet JP, Gattone VH 2nd: Autosomal-dominant polycystic kidney disease in the rat. Kidney Int 1993;43:522–534.
31 Gattone VH 2nd, Tourkow BA, Trambaugh CM, Yu AC, Whelan S, Phillips CL, Harris PC, Peterson RG: Development of multiorgan pathology in the wpk rat model of polycystic kidney disease. Anat Rec A Discov Mol Cell Evol Biol 2004;277:384–395.
32 Kranzlin B, Schieren G, Gretz N: Azotemia and extrarenal manifestations in old female Han:Sprd (cy/+) rats. Kidney Int 1997;51:1160–1169.
33 Gabow PA, Johnson AM, Kaehny WD, Kimberling WJ, Lezotte DC, Duley IT, Jones RH: Factors affecting the progression of renal disease in autosomal-dominant polycystic kidney disease. Kidney Int 1992;41:1311–1319.
34 Gretz N, Ceccherini I, Kranzlin B, Kloting I, Devoto M, Rohmeiss P, Hocher B, Waldherr R, Romeo G: Gender-dependent disease severity in autosomal polycystic kidney disease of rats. Kidney Int 1995;48:496–500.
35 Stringer KD, Komers R, Osman SA, Oyama TT, Lindsley JN, Anderson S: Gender hormones and the progression of experimental polycystic kidney disease. Kidney Int 2005;68:1729–1739.
36 Gonzalo A, Gallego A, Rivera M, Orte L, Ortuno J: Influence of hypertension on early renal insufficiency in autosomal dominant polycystic kidney disease. Nephron 1996;72:225–230.
37 Zerres K, Rudnik-Schoneborn S, Senderek J, Eggermann T, Bergmann C: Autosomal recessive polycystic kidney disease (ARPKD). J Nephrol 2003;16:453–458.
38 Chapman AB, Johnson AM, Rainguet S, Hossack K, Gabow P, Schrier RW: Left ventricular hypertrophy in autosomal dominant polycystic kidney disease. J Am Soc Nephrol 1997;8:1292–1297.
39 Schrier R, McFann K, Johnson A, Chapman A, Edelstein C, Brosnahan G, Ecder T, Tison L: Cardiac and renal effects of standard versus rigorous blood pressure control in autosomal-dominant polycystic kidney disease: results of a seven-year prospective randomized study. J Am Soc Nephrol 2002;13:1733–1739.
40 Fall PJ, Prisant LM: Polycystic kidney disease. J Clin Hypertens 2005;7:617–625.
41 Valvo E, Gammaro L, Tessitore N, Panzetta G, Lupo A, Loschiavo C, Oldrizzi L, Fabris A, Rugiu C, Ortalda V, et al.: Hypertension of polycystic kidney disease: Mechanisms and hemodynamic alterations. Am J Nephrol 1985;5:176–181.
42 Danielsen H, Nielsen AH, Pedersen EB, Herlevsen P, Kornerup HJ, Posborg V: Exaggerated natriuresis in adult polycystic kidney disease. Acta Med Scand 1986;219:59–66.
43 Doulton TW, Saggar-Malik AK, He FJ, Carney C, Markandu ND, Sagnella GA, MacGregor GA: The effect of sodium and angiotensin-converting enzyme inhibition on the classic circulating renin-angiotensin system in autosomal-dominant polycystic kidney disease patients. J Hypertens 2006;24:939–945.
44 Sorensen SS, Glud TK, Sorensen PJ, Amdisen A, Pedersen EB: Change in renal tubular sodium and water handling during progression of polycystic kidney disease: relationship to atrial natriuretic peptide. Nephrol Dial Transplant 1990;5:247–257.
45 Hackenthal E, Paul M, Ganten D, Taugner R: Morphology, physiology, and molecular biology of renin secretion Physiol Rev 1990;70.
46 Skott O: Renin. Am J Physiol Regul Integr Comp Physiol 2002;282:R937–R939.
47 Harrap SB, Dominiczak AF, Fraser R, Lever AF, Morton JJ, Foy CJ, Watt GC: Plasma angiotensin II, predisposition to hypertension, and left ventricular size in healthy young adults. Circulation 1996;93:1148–1154.
48 Thananopavarn C, Golub MS, Eggena P, Barrett JD, Sambhi MP: Angiotensin II, plasma renin and sodium depletion as determinants of blood pressure response to saralasin in essential hypertension. Circulation 1980;61:920–924.
49 Kosunen KJ, Pakarinen AJ, Kuoppasalmi K, Adlercreutz H: Plasma renin activity, angiotensin II, and aldosterone during intense heat stress. J Appl Physiol 1976;41:323–327.
50 Ayers CR, Katholi RE, Vaughan EDJ, Carey RM, Kimbrough HMJ, Yancey MR, Morton CL: Intrarenal renin-angiotensin-sodium interdependent mechanism controlling postclamp renal artery pressure and renin release in the conscious dog with chronic one-kidney Goldblatt hypertension. Circ Res 1977;40:238–242.
51 Liard JF, Cowley AWJ, McCaa RE, Guyton AC: Renin, aldosterone, body fluid volumes, and the baroreceptor reflex in the development and reversal of goldblatt hypertension in conscious dogs. Circ Res 1974;34:549–560.

52 Dzau VJ, Colucci WS, Hollenberg NK, Williams GH: Relation of the renin-angiotensin-aldosterone system to clinical state in congestive heart failure. Circulation 1981;63:645–651.
53 Watkins LJ, Burton JA, Haber E, Cant JR, Smith FW, Barger AC: The renin-angiotensin-aldosterone system in congestive failure in conscious dogs. J Clin Invest 1976;57:1606–1617.
54 Pedersen KM, Pedersen HD, Haggstrom J, Koch J, Ersboll AK: Increased mean arterial pressure and aldosterone-to-renin ratio in Persian cats with polycystic kidney disease. J Vet Intern Med 2003;17:21–27.
55 Hollenberg NK: Aldosterone in the development and progression of renal injury. Kidney Int 2004;66:1–9.
56 Cerasola G, Vecchi M, Mule G, Cottone S, Mangano MT, Andronico G, Contorno A, Parrino I, Renda F, Pavone G: Sympathetic activity and blood pressure pattern in autosomal dominant polycystic kidney disease hypertensives. Am J Nephrol 1998;18:391–398.
57 Roysommuti S, Mozaffari MS, Wyss JM: Insulin-exacerbated hypertension in captopril-treated spontaneously hypertensive rats: role of sympathoexcitation. Can J Physiol Pharmacol 2003;81:1036–1041.
58 Bergamaschi C, Campos RR, Schor N, Lopes OU: Role of the rostral ventrolateral medulla in maintenance of blood pressure in rats with Goldblatt hypertension. Hypertension 1995;26:1117–1120.
59 Korner PI, Angus JA: Structural determinants of vascular resistance properties in hypertension: haemodynamic and model analysis. J Vasc Res 1992;29:293–312.
60 McKinley MJ, Allen AM, Burns P, Colvill LM, Oldfield BJ: Interaction of circulating hormones with the brain: the roles of the subfornical organ and the organum vasculosum of the lamina terminalis. Clin Exp Pharmacol Physiol Suppl 1998;25:S61–67.
61 Fitch GK, Weiss ML: Activation of renal afferent pathways following furosemide treatment. II. Effect of angiotensin blockade. Brain Res 2000;861:377–389.
62 Converse RL, Jacobsen TN, Toto RD, Jost CMT, Cosentino F, Tarazi F, Victor GG: Sympathetic overactivity in patients with chronic renal failure. N Engl J Med 1992;327:1912–1918.
63 Ciriello J, de Oliveira CV: Renal afferents and hypertension. Curr Hypertens Rep 2002;4:136–142.
64 Ye S, Zhong H, Yanamadala V, Campese VM: Renal injury caused by intrarenal injection of phenol increases afferent and efferent renal sympathetic nerve activity. Am J Hypertens 2002;15:717–724.
65 Campese VM, Kogosov E: Renal afferent denervation prevents hypertension in rats with chronic renal failure. Hypertension 1995;25:878–882.
66 Tao Y, Kim J, Schrier RW, Edelstein CL: Rapamycin markedly slows disease progression in a rat model of polycystic kidney disease. J Am Soc Nephrol 2005;16:46–51.